Bull. Mater. Sci. (2018) 41:13
https://doi.org/10.1007/s12034-017-1526-6

Dielectric properties study of surface engineered nanoTiO_2/epoxy composites

SASIDHAR SIDDABATTUNI[1,*], SRI HARSHA AKELLA[1], ABILASH GANGULA[1], SIVAKUMAR BELLIRAJ[1] and L A AVINASH CHUNDURI[2]

[1]Department of Chemistry, Sri Sathya Sai Institute of Higher Learning, Vidyagiri, Prasanthi Nilayam, Puttaparthi 515134, India

[2]Department of Physics, Sri Sathya Sai Institute of Higher Learning, Vidyagiri, Prasanthi Nilayam, Puttaparthi 515134, India

*Author for correspondence (siddabattunisasidhar@sssihl.edu.in)

MS received 2 August 2016; accepted 25 May 2017; published online 2 February 2018

Abstract. Nanodielectrics are promising materials that can efficiently store a large amount of electrical energy that are desirable for many electronic and power devices. Control of polymer–particle interface in nanodielectrics is very critical in not only obtaining the improved quality of dispersion but also in altering the dielectric properties. Various surface modifying agents with linear (alkyl), aromatic (phenyl) and extended aromatic (naphthyl) chemical nature were employed at the epoxy–nanoTiO_2 interface. All the surface-modifying agents were successful in passivating the nanoparticles surface and in obtaining the improved quality of polymer–particle dispersion and improved glass transition temperature comparatively. However, all the surface modifiers were not successful in obtaining the improved dielectric properties of the nanodielectrics, especially dielectric breakdown resistance. Only the extended aromatic group at the polymer–particle interface, which is more electron withdrawing in electronic nature than phenyl and alkyl structures, was successful in improving the dielectric breakdown resistance. Thus, the choice of surface-modifying agent based on its chemical and electronic nature is very important in optimizing the dielectric properties of nanodielectrics. Naphthyl phosphate-modified nanoTiO_2–epoxy composite films of ~90–100 μm thick at 5 vol% particle concentration yielded higher dielectric breakdown resistance than pure epoxy polymer and thereby resulted in about 90% higher electrical energy storage density than the pure epoxy film.

Keywords. Nanodielectrics; interface; organophosphate; dielectric breakdown strength; electron-withdrawing; energy density.

1. Introduction

Dielectric materials are used to control and store electrical charges and electric energies that play a key role in modern electronics and electric power systems [1]. The maximum energy density (U_{max}) (energy stored per volume) in a linear dielectric material is limited to equation (1), where ε_r is the dielectric constant or permittivity of the material, ε_o (8.854×10^{-12} F m^{-1}) is the permittivity of free space and E_b is the dielectric breakdown strength (DBS). Both a larger permittivity and greater breakdown strength improve electric energy storage [2].

$$U_{max} = \frac{1}{2}\varepsilon_o \varepsilon_r E_b^2 \quad (1)$$

Ceramic-based dielectric materials, which are inorganic in nature, are usually known to possess large dielectric permittivity, but they are scarce by their relatively small DBS, poor processability and mechanical properties due to high sintering temperature and porosity. On the other hand, polymer-based dielectric materials, which are organic in nature, usually possess high DBS, low dielectric losses, excellent mechanical properties and processability but suffer from smaller dielectric permittivity [2–4]. Miniaturization and the current increasing need and demand for high power density, high voltage capacitors and power-storage devices have stimulated the use of polymer nanocomposite dielectric materials, known as nanodielectrics that combine the advantages of both high DBS from polymer fractions and high permittivity from ceramic nanoparticles fraction of the composite to obtain improved or enhanced dielectric properties [5–10].

The most distinctive feature of nanodielectrics in comparison with conventional microcomposites is the extremely high surface area available between the nanoparticles and the polymer matrix. Smaller the size of the embedded nanoparticles, larger is the surface area to volume ratio, which leads to larger interface regions [11]. Thus, control of interface is very important as the properties of the nanodielectrics are often influenced by the large interfacial regions. Failure to control the interface results in aggregation or agglomeration of nanoparticles in polymer matrix, which leads to

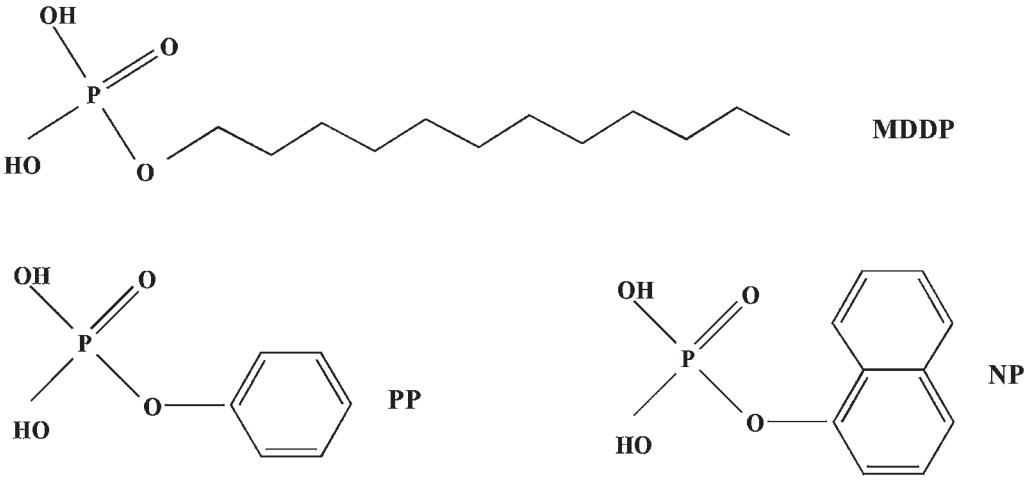

Figure 1. Molecular structures of organophosphate ligands: monododecylphosphate (MDDP), phenyl phosphate (PP) and 1-naphthyl phosphate (NP) used to modify the surface of nano-TiO_2.

detrimental effects on the dielectric properties due to poor film quality and inhomogeneities [7,12]. In other words, interfaces that can conduct charges are created when dispersing high surface energy ceramic particles into a low surface energy polymer, which can thus produce low breakdown resistance and also make uniform dispersion of the particles problematic [13]. Thus, without controlling the interface, the advantage of 'nano' effect cannot be fully utilized in designing the nanodielectrics with desired dielectric properties.

Treating the surface of nanoparticles using suitable surfactants or surface coupling agents is one way of controlling the interface to obtain proper compatibility between the ceramic nanoparticles and polymers. A stable and complex organic oxide interface can be achieved by treating the ceramic nanoparticles' surface with various types of surface coupling agents like phosphates, phosphonates or silanes [13,14]. These surface-treated ceramic nanoparticles can provide improved dispersion and film quality that has potential to improve the dielectric breakdown strengths when added to polymer matrices compared with very leaky interfaces of nanodielectrics without any surface treatment [7,13].

In our earlier work, it was demonstrated that surface modification is not only important in achieving good quality of dispersion in nanodielectrics, but also very crucial in altering and enhancing the dielectric properties of the nanodielectrics, based on the electronic nature of chemical or functional groups available at the interface [15]. However, only aromatic organophosphate ligands with and without additional functional groups were utilized to derive the structure–property relationship. To further understand the influence of polymer–particle interfacial chemical nature on the dielectric properties of nanodielectrics, in this present work, we employed linear, aromatic and extended aromatic organic groups containing organophosphate ligand molecules without any additional functional groups at the interface of nanoTiO_2 and epoxy resin. Figure 1 shows the chemical structures of organophosphate ligands that were examined as surface-modifying agents.

2. Experimental

Commercially available nanoTiO_2 powder (> 99%, 10–25 nm APS and 200–240 $m^2\ g^{-1}$) was obtained from US Research Nano Materials Inc., Texas, USA and used as is in the preparation of nanodielectrics and surface functionalization. BYK-w-9010 (a proprietary co-polymer mixture with acidic groups) was provided by BYK-Chimie. Organophosphate surface-modifying agents, monododecylphosphate (MDDP) and phenyl phosphate (PP), were obtained from TCI Chemicals (India) Pvt. Ltd. and 1-naphthyl phosphate (NP) was obtained from Sigma Aldrich, USA. Epoxy resin system, DER 332 and its curing agent, tetraethyltetramine (TETA) were obtained from Sigma Aldrich, USA.

In a typical surface modification reaction, TiO_2 nanoparticles were first dispersed in a suitable solvent. Organophosphate ligand, approximately 10–15 wt% of particle mass was mixed with the dispersion and stirred at reflux conditions for 18–24 h. The surface-modified nanoTiO_2 powder was then isolated and purified by washing through repeated centrifugation and re-dispersion in solvent for 4–5 times to remove any excess and/or physisorbed ligands. The surface-treated TiO_2 nanoparticles were dried thoroughly at 160°C for 6–10 h.

For obtaining the electrostatic maps of the surface modifiers, the ligand structures were constructed using GaussView 5.0 and was optimized using AVDZ (augmented double zeta potential), followed by a geometry optimization using the Density Functional Theory, with a basis set of B3LYP/6-31G(d) method using Gaussian 09 software.

The powders, modified and unmodified, were analysed by a thermogravimetric analyser (TGA), X-ray photoelectron spectroscopy (XPS) and impedance spectroscopy through

powder slurry technique in Maxwell liquid as described elsewhere [16]. Nanodielectric films were made by first dispersing surface-treated TiO_2 nanoparticles into epoxy resin (DER 332) via a planetary ball mill (Retsch, PM 100 Model, Germany) for ~15 h. BYK-w-9010 was added to unmodified TiO_2 nanoparticle dispersion into epoxy as an experimental control to compare a dispersed particle composite against a self-dispersing (surface modified) particle, wherein the particle uses the bound surface groups to aid its dispersion. The stoichiometric amount of curing agent, TETA, was added to the ball-milled nanoTiO_2–epoxy dispersion and the uncured liquid composite was stirred for 5 min and degassed before casting and curing the films. Films of the uncured liquid composite were applied to freshly exposed, polished 0.8 mm thick polished copper substrate obtained from the Steel Emporium, Mumbai. The composite films were allowed to cure at 60°C for 20 h followed by 150°C for 2 h.

The completely cured nanodielectric films prepared were characterized using differential scanning calorimetry (DSC), scanning electron microscopy (SEM), electrical impedance and dielectric breakdown strength. Film thicknesses were measured with a Mitutoyo 0293-340 micrometer and then the thickness of the copper substrate was subtracted.

Glass transition temperature (T_g) of all the nanocomposite films were assessed in a NetzschDSC 200 F3 Maia Thermal Analyzer after a preliminary thermal anneal stage (10°C min^{-1}, from ambient to 100°C, cooled to 0°C temperature) by scanning temperature from ambient to 150°C. Glass transition temperatures are reported using the inflection point of the transition. The film morphology was imaged by using Ultra 55FE-SEM (Carl Zeiss AG) after sputter coating the dielectric films with a gold-palladium coating. Brightness and contrast of the images were adjusted using the ImageJ software. Parallel-plate capacitors were fabricated by depositing circular (50 mm^2) silver (AG paste MS-5000, Gredmann, Taiwan) top electrodes onto the nanocomposite thin films. Frequency dependent capacitance and tan δ (dielectric loss) were measured using HP 4294A Impedance Analyzer (Agilent Technologies Inc., Santa Clara, CA) at a frequency range from 1 Hz to 1 MHz at room temperature. Reported relative dielectric constant used for energy density calculation was calculated according to capacitance measured at 10 kHz. DBS measurements were made by applying DC voltage across the films using a high voltage generator (Power Electricals, Nasik, India), with a maximum ramp rate of 500 V s^{-1} until the point of film failure. A pin electrode was applied by light spring tension to the surface of the composite, which served as the electrical ground. The DBS data obtained were analysed using Weibull failure analysis [equation (2)] method as described elsewhere [15]. In equation 2, an empirical failure probability (P_F) is equated to median-ranked positioning [equation (3)] of sample occurrence within a test population and E are measured DBS values. In equation (3), i is the index (1, 2, 3, … n) and n is the sample size. The measured n breakdown values (E) are reordered in ascending order and then the probability failure for each E is given from the positioning equation. The discrete measurements are merged from multiple measurements of multiple samples' results and are thus expected to show population statistical DBS. The scale parameter, α, represents the field intensity corresponding to a 63.2% breakdown probability (P_F). β shows the dispersion and consistency of the DBS values.

$$\log[-\ln\{1 - P_F(E)\}] = \beta \log E - \beta \log \alpha \quad (2)$$

$$P_F(i, n) = (i - 0.5)/(n + 0.25) \quad (3)$$

3. Results and discussion

After treating the surface of nanoTiO_2 particles using organophosphate coupling agents, the nanopowders were first assessed for the quality and quantity of surface modification. In this regard, TGA and XPS measurements obtained from the surface modified and the unmodified TiO_2 nanopowders are shown in table 1. At above 200°C, a significant weight loss was observed (refer to figure 2) for the organophosphate modified nanoTiO_2. This weight loss was attributed mainly to the thermal decomposition and volatilization of organic residues from the organic groups present on the surface of TiO_2 as a result of surface modification [15,16]. Based on the organic weight loss, surface group density of the surface modifier present on the nanoparticles surface was then calculated using the particle surface area and mass of TiO_2 and the organic molecular weight of the surface modifier using similar method that was reported earlier for surface modified metal oxide

Table 1. TGA and XPS characterization data of surface-treated nanoTiO_2 powders in comparison to untreated nanoTiO_2 powders.

	TGA		XPS (atomic percent)			
Powder	Organic weight loss (%)	Surface group density (groups nm^{-2})	C 1s	Ti 2p	O 1s	P 2p
NanoTiO_2	0	—	37.66	3.07	59.27	0.00
MDDP-treated nanoTiO_2	8.88	1.11	34.89	9.58	53.05	2.48
PP-treated nanoTiO_2	4.3	0.83	42.23	6.44	49.37	1.96
NP-treated nanoTiO_2	2.87	0.41	45.54	4.80	47.34	2.32

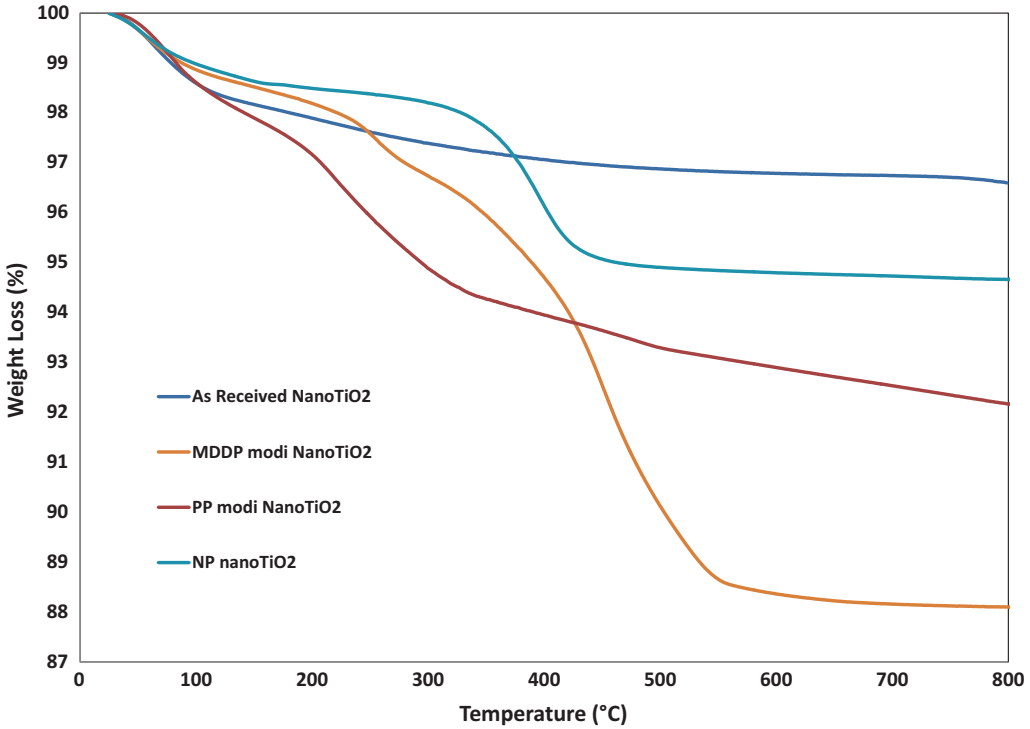

Figure 2. TGA analysis of surface-modified and unmodified TiO_2 nanoparticles.

particles [17]. TGA measurements of MDDP and PP-treated TiO_2 nanoparticles showed surface group density of about one organophosphate molecule per nm^2 area of nanoTiO_2, which is about one-fourth that of the theoretical surface group density of organophosphonate groups per nm^2 for highly ordered self-assembled monolayers [18]. A polycrystalline nature of TiO_2 nanoparticles surface and the possible multidentate bonding of the surface modifiers on nanoparticles surface are held responsible for relatively less order or less surface group density compared to theoretical assumption [15,16]. Organic weight loss of NP-treated TiO_2 nanoparticles resulted in the surface group density of only about half an organophosphate molecule per nm^2, which is attributed mainly to the pronounced steric effect offered by the aryl groups (naphthyl) of NP surface modifier. XPS measurements indicate the introduction of phosphorus groups on the surface-modified nanoTiO_2 samples. The surface-modified powders mainly showed bridged phosphate oxygen corresponding to the phosphonyloxygen (P=O), phosphoryl oxygen (P–O) and R–O–P bonds, where R is alkyl or aryl (phenyl, naphthyl) carbon of the organophosphate ligands at the regions ranging from 532 to 534 eV [16].

After both TGA and XPS measurements supported a consistent, chemically strong surface bonding by organophosphate ligands on nanoTiO_2, nanopowders were utilized for synthesizing polymer–particle nanocomposites in the epoxy matrix. Surface modification of nanoTiO_2 assisted in improved dispersion of nanoparticles in epoxy matrix when compared with unmodified nanoTiO_2, as evident from the FE-SEM images of the nanocomposite films at 5 vol% particle concentration (figure 3). SEM images of unmodified TiO_2 nanoparticle composites exhibited pinhole surface defects and poor quality of dispersion. In contrast, nanocomposites with all organophosphate ligand-modified TiO_2 nanoparticles yielded improved dispersion quality. Quality of dispersion was not observed to change significantly for different organophosphate ligands-employed to modify the TiO_2 nanoparticles surface. Therefore, any changes in the subsequent thermal and dielectric studies of the polymer nanocomposite films between the unmodified and surface modified nanoparticles has to be due to the polymer–particle interfacial differences.

Glass transition temperature (T_g) of polymer nanocomposites, obtained by DSC, is related to the free volume of the polymer chains as described by the Williams–Landel–Ferry theory and the interaction strength between the polymer and particle interface [19,20]. Blum *et al* have studied how particle curvature, surface adsorption and composition influence the polymer-free volume observed as changes in glass transition temperature and deuterium nuclear magnetic resonance relaxation [21,22]. In our present study, pristine epoxy polymer showed a T_g inflection point of about 125°C, while unmodified nanoparticle composites with commercial phosphate ester dispersant showed a depressed T_g inflection point of about 116°C (table 2 and figure 4), a fairly large decrease of about 9°C. This decrease in T_g, which is typical to polymer nanocomposites as compared to pure polymer, is caused by the nanoparticle radius of curvature increasing the free

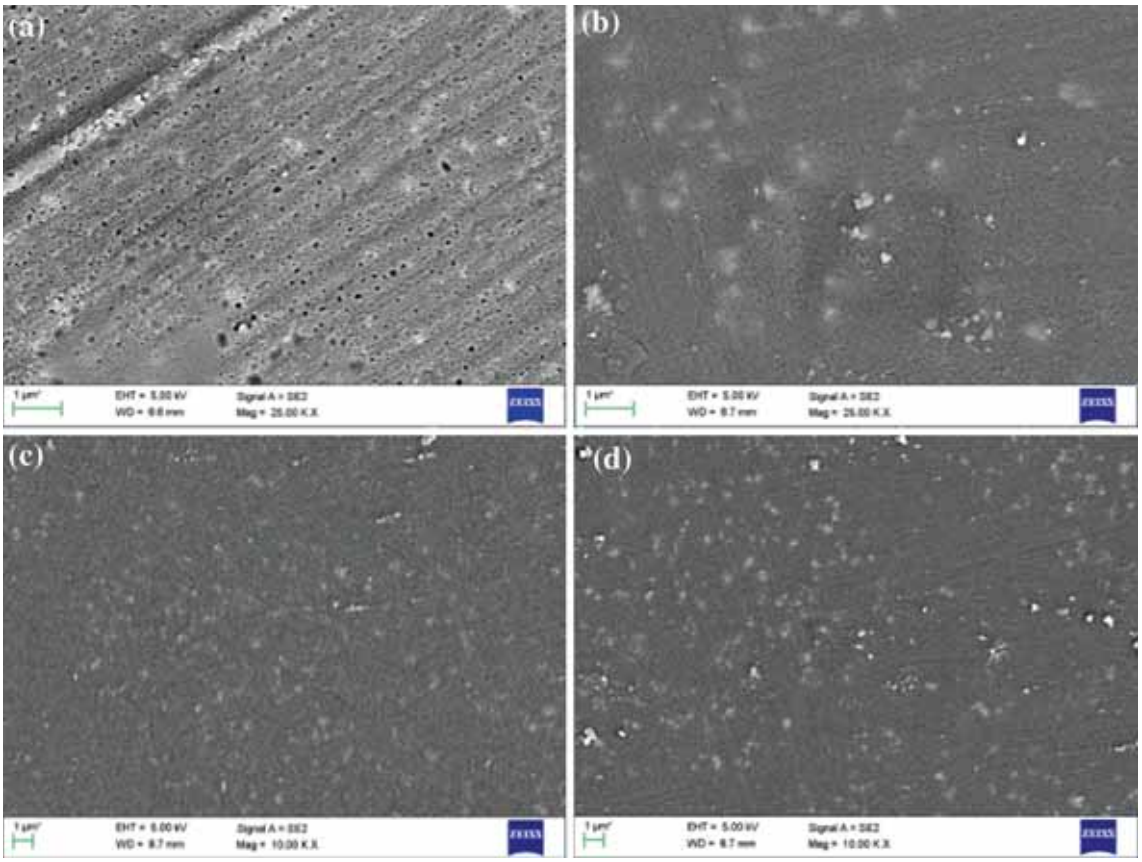

Figure 3. FE-SEM images of 5 vol% nanocomposite films: (**a**) untreated nanoTiO_2–epoxy (with BYK-w-9010), (**b**) MDDP-treated nanoTiO_2–epoxy, (**c**) PP-treated nanoTiO_2–epoxy and (**d**) NP-treated nanoTiO_2–epoxy.

volume of the polymer chains [21]. This decrease in T_g also suggests weakly bonded polymer–particle interface caused by the increase in the free volume of the polymer chains at the interface [13]. However, when organophosphate ligand-treated nanoparticles are incorporated in the epoxy polymer matrices, T_g is either retained to that of bulk pure polymer or even further improved (table 2 and figure 4). This improvement in the T_g for all surface-treated nanoparticles–polymer composites is mainly attributed to a stronger interface caused by the phosphate groups that are capable of forming strong, stable and complex oxide bonding on the nanoparticles surface. This strong interfacial bonding restricted the polymer chain mobility at the interface, thereby reducing the local free volume and improving the overall T_g.

Free volume has influence on the dielectric breakdown resistance and have previously evidenced that greater free volume due to weak polymer–particle interface reduces dielectric breakdown resistance [15,23,24]. Our results for DBS data obtained and analysed using Weibull failure analysis method, which has been frequently adopted for the investigation of dielectric breakdown of different material systems [25], also suggests the same. The DBS measurements were reproduced using multiple samples and thus show the Weibull distribution intercept (E) expected over multiple measurements. An unmodified nanoTiO_2 filled nanocomposite with lower T_g showed lower DBS compared to the pure epoxy polymer (table 2 and figure 5). However, all surface modified nanoTiO_2 nanocomposites with T_g similar to pure polymer or even better than pure polymer due to stronger interface and with improved quality of dispersion compared to unmodified nanoTiO_2 did not yield higher DBS compared to pure epoxy polymer. NP-modified nanoTiO_2 nanocomposite alone showed significant improvement in DBS when compared to pure epoxy and other surface-modified nanoTiO_2 nanocomposites. This difference in DBS for various surface-treated nanoTiO_2 is mainly attributed to the difference in the chemical nature of polymer–particle interface of the nanocomposites.

If we analyse the type of surface modifiers employed for treating the nanoTiO_2 surface, MDDP has alkyl (linear) backbone chain, PP has aromatic ring and NP has extended aromatic ring. Alkyl group of MDDP is traditionally known to be electron donating through inductive effect, whereas phenyl group and aryl group (Naphthyl) of PP and NP can be either electron donating or electron withdrawing due to strong resonance effects [26]. DBS results of the polymer nanocomposites suggest that the polymer–particle interface possessed higher dielectric breakdown resistance when aryl group of

Table 2. DSC and dielectric properties characterization data of 5 vol% epoxy–nanoTiO_2 composites compared to pure polymer.

Dielectric sample (~90–100 μm thickness)	T_g (°C)	DBS (V μm^{-1})	Dielectric constant at 10 kHz	Dielectric loss at 1 kHz	Dielectric loss at 10 kHz	Max. energy density (J cm^{-3})
Pure epoxy	125	102.1	4.49	< 0.029	< 0.042	0.21
NanoTiO_2/epoxy (5PVC)	116	91.1	6.30	< 0.036	< 0.046	0.23
NP-treated nanoTiO_2/epoxy (5PVC)	128	120.3	6.27	< 0.032	< 0.042	0.40
PP-treated nanoTiO_2/epoxy (5PVC)	129	95.9	6.33	< 0.030	< 0.041	0.26
MDDP-treated nanoTiO_2/epoxy (5PVC)	124	84.8	6.39	< 0.033	< 0.043	0.20

NP is present at the interface as compared to phenyl group of PP and alkyl group of MDDP. The order of increase in the dielectric breakdown resistance was observed to be alkyl < phenyl < aryl.

Impedance spectroscopy results of nanoparticles of various surface-modified nanoTiO_2 powders in comparison to unmodified nanoTiO_2 powder using powder slurry technique supports the above argument (figure 6 and table 3) based on the electrical resistivity differences observed for different surface modifiers. The complex impedance spectra (Z'' *vs.* Z', where Z' and Z'' are real and imaginary parts of the complex impedance) of the particles slurries in a Maxwell liquid, butoxyethanol, were subjected to equivalent circuit modelling to deconvolute the solvent element contributions from particle element contributions using two RC elements (figure 6). Four parameters, high-frequency resistance (R1) and capacitance (C1) corresponding to the liquid portion of the slurries and low-frequency resistance (R2) and constant phase element (CPE2) corresponding to the particle portion of the slurries obtained for each impedance spectrum and their calculated dielectric permittivities of individual components of the slurries are reported in table 3. The equivalent circuit modelling of the impedance spectroscopy data showed that the electrical resistance (R2) and the corresponding electrical resistivity (calculated from R2 using the formula $\rho = R \times AL^{-1}$, where A and L are the area and separation distance of the sample impedance measurement cell) of surface-modified nanoTiO_2 was either lowered or improved than unmodified nanoTiO_2. MDDP-treated nanoTiO_2 was observed to result in 50% reduction in the electrical resistivity, whereas PP- and NP-treated nanoTiO_2 were observed to result in about 100 and 150% increase in the electrical resistivity as compared to untreated nanoTiO_2. Improvement in the electrical resistivity of particle resistivity was observed to be in the order of MDDP < PP < NP [16]. This difference in the electrical resistivity is attributed to the difference in the chemical nature of ligands present on the nanoTiO_2 surface. Hence, the choice of chemical nature of ligands employed for surface passivation of metal oxide nanoparticles plays an important role in altering the particle surface electrical resistivity and their DBS in polymer nanocomposites. Surface passivated nanoTiO_2 powders yielded reliable and reproducible permittivity values in the range of 70–80 compared to untreated nanoTiO_2 powder. The choice of an organic functional group did not seem to influence the dielectric permittivity of nanoTiO_2 to a significant extent [16].

We hereby present that the electronic nature of the particle's surface, based on the type of functional groups of the organophosphate ligand, correlated with improvements observed in the DBS results. Electrostatic potential (ESP) maps of various functional groups containing organophosphate surface modifiers (figure 7) suggest that the alkyl chain of MDDP is electron-donating and thus the alkyl chain possessed slightly electropositive charge (observed as blue colour in MDDP ESP map) after donating its electrons to the oxygen of R–O–P link of phosphate ester through induction effect.

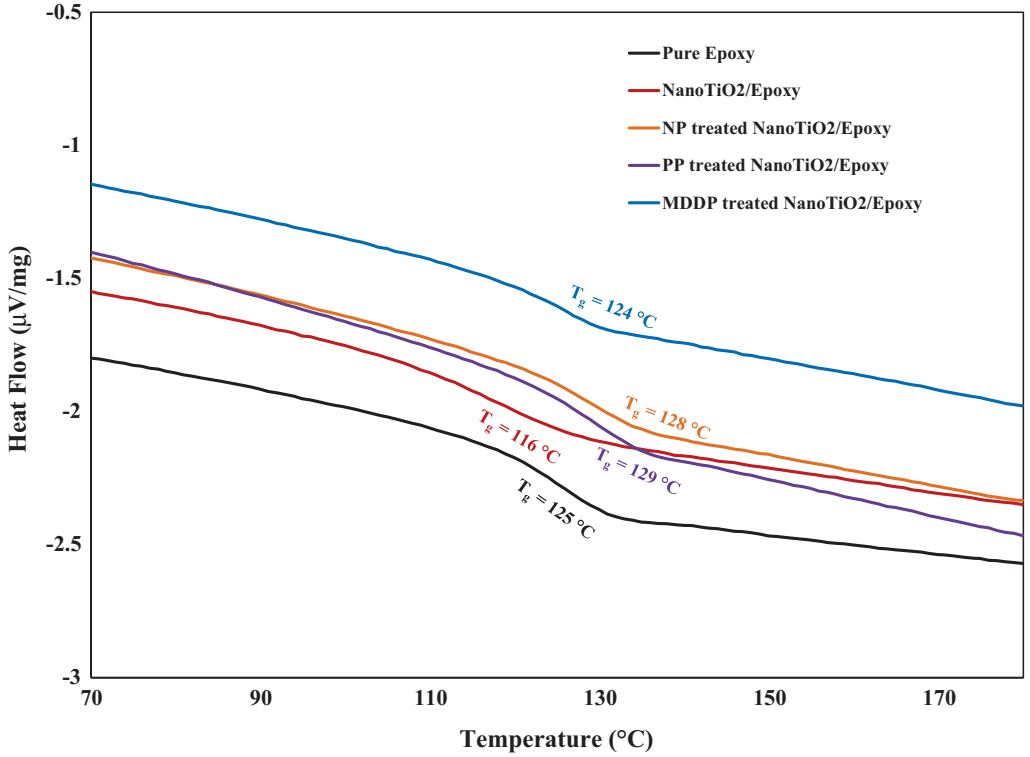

Figure 4. DSC plot of the epoxy polymer in comparison with the 5 vol% nanoTiO$_2$–epoxy composites (T_g values are based on inflection point).

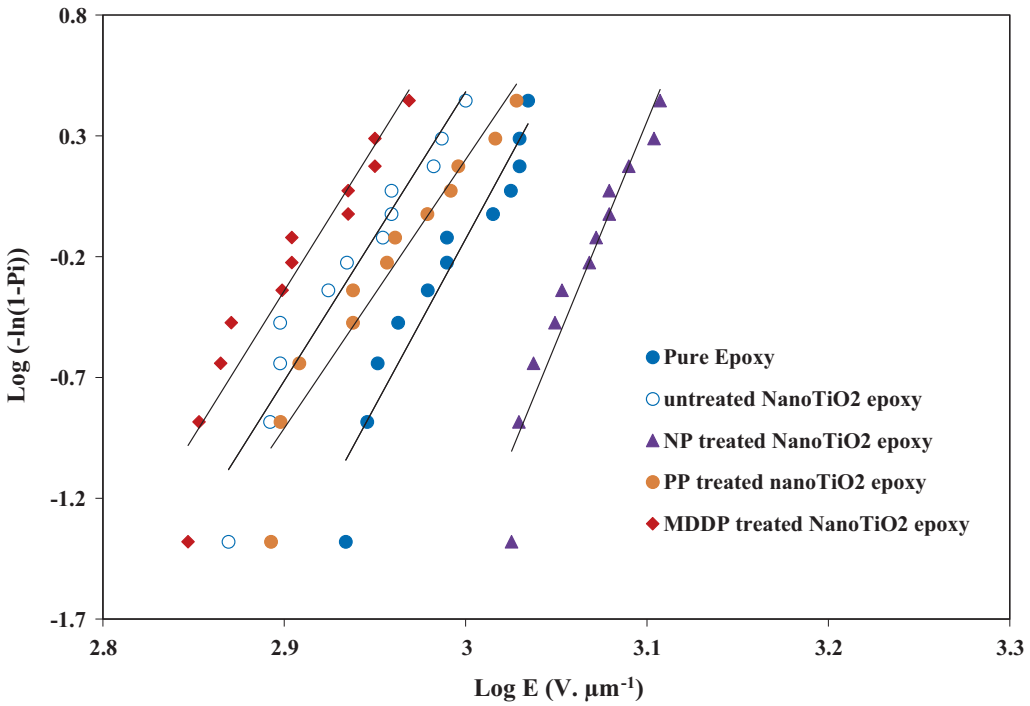

Figure 5. Weibull plot of DBS measurements for 5 vol% epoxy–nanoTiO$_2$-based dielectric films.

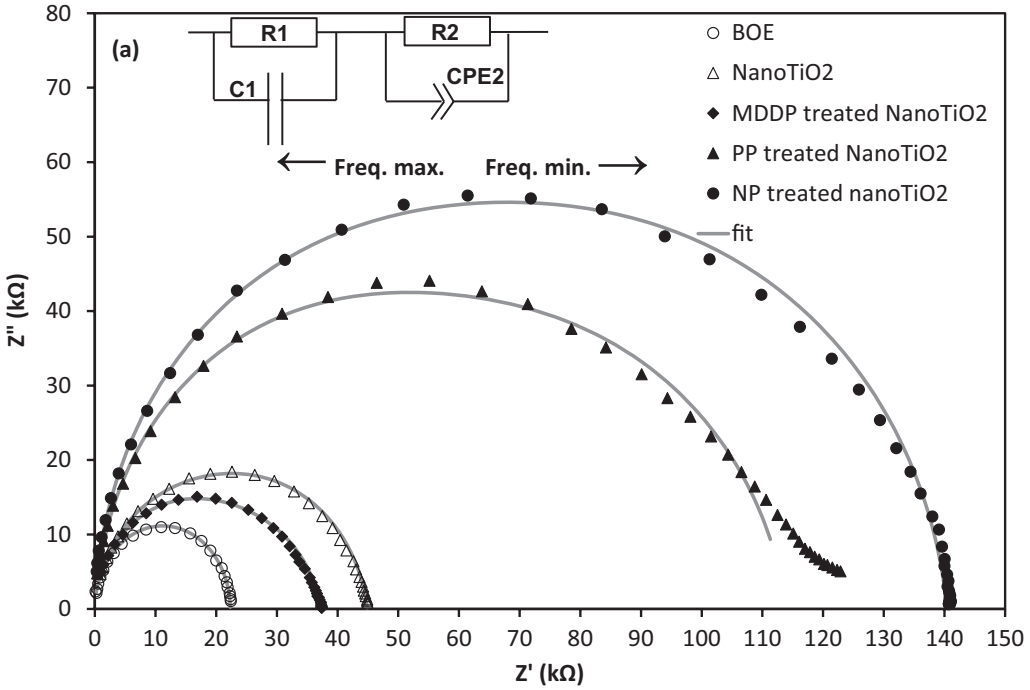

Figure 6. Impedance spectra of 20 vol% nanoTiO_2-based powders.

Table 3. Fitting parameters of the impedance data and the permittivity values of the nanoTiO_2 slurries in BOE at 20 vol%.

Sample	R1 (kΩ)	C1 (F)	R2 (kΩ)	CPE2-T (F)	CPE2-P	C2 (F)	ε_r^a	ε_r^b
BOE	23.9	3.1E−11	—	—	—	—	10.7	—
NanoTiO_2	10.9	9.9E−11	33.9	3.27E−10	0.90	9.7E−11	42.1	41.3
MDDP nanoTiO_2	17.4	6.1E−11	19.8	8.94E−10	0.87	1.7E−10	25.7	72.3
PP nanoTiO_2	46.9	6.6E−11	67.0	7.25E−10	0.88	1.9E−10	28.1	80.6
NP nanoTiO_2	56.7	6.3E−11	83.7	3.99E−10	0.92	1.6E−10	26.7	70.7

[a]Permittivity of liquid component of the slurry.
[b]Permittivity of particulate component of the slurry.

Phenyl group and aryl group of PP and NP appeared to be electron-withdrawing in nature through resonance effects and thus the phenyl and naphthyl rings possessed negative charge (observed as red colour in the NP and PP ESP maps) after withdrawing electrons from the oxygen of R–O–P link of phosphate ester. Based on the ESP maps, naphthyl ring is observed to be more electron-withdrawing than phenyl ring, which is attributed mainly due to the presence of several canonical structures in naphthyl ring compared to phenyl ring. Thus, the NP surface modifier with several canonical structures in its phenyl ring can be held responsible for more electrical resistivity and thereby, greater DBS results obtained for NP-treated nanoTiO_2–epoxy composites than those of PP and MDDP surface modifiers.

Aryl (phenyl, naphthyl) groups which contains π (pi) electrons are known to be more polarizable than the simple alkyl group [27]. However, impedance measurements of various surface-treated nanoTiO_2 polymer nanocomposites did not show any appreciable difference in dielectric permittivity at 5 vol% particle concentration (table 2) as those polarizability differences are very small. The dielectric permittivities of the polymer nanocomposites were observed to be more or less similar. Comparatively, dielectric loss data for surface-modified nanoTiO_2 polymer nanocomposites was observed to be lower than the unmodified nanoTiO_2 polymer nanocomposites mainly due to the stronger polymer–particle interface and improved quality of dispersion. Owing to the improved DBS of NP-treated nanoTiO_2–epoxy composite than the pure epoxy polymer, the maximum electrical energy storage density of the NP-treated nanoTiO_2–epoxy composite at 5 vol% particle concentration, calculated from equation (1), was observed to be more than 90% higher than the pure epoxy polymer (table 2). Only slight improvement or no improvement in the maximum electrical energy storage density was observed for the PP- and MDDP-treated nanoTiO_2–epoxy composites when compared with pure epoxy.

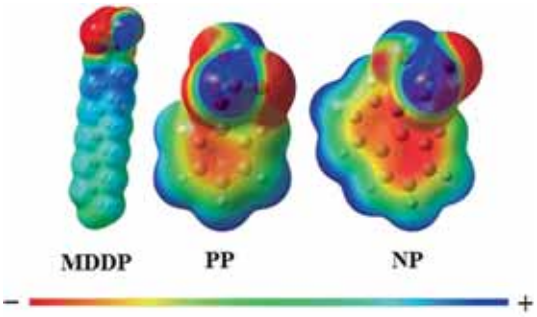

Figure 7. Electrostatic potential maps of surface modifiers obtained from DFT modelling. Red colour indicates negative charge, whereas blue colour indicates positive charge.

4. Conclusions

Use of interfacial coupling agents is an effective approach to improve the quality of dispersion and polymer–particle interaction in a nanocomposite dielectric film. However, all interfacial coupling agents with improved interaction between polymer and particle does not necessarily result in improved dielectric properties of their nanodielectrics. Proper selection of interfacial coupling agents based on the electronic and chemical nature of the functional groups present at the polymer–particle interface is required to optimize the dielectric properties of the nanodielectrics. We have demonstrated that the electron-withdrawing nature of functional groups is preferable to improve the dielectric properties, especially dielectric breakdown resistance. Our comparison study between alkyl (of MDDP), aromatic (of PP) and extended aromatic (of NP) chemical nature at the polymer–particle interface suggested that the extended aromatic ring, which is more electron-withdrawing in nature than aromatic and alkyl groups resulted in improved dielectric breakdown resistance and improved glass transition temperature than the pure epoxy polymer at 5 vol% particle concentration. NP-treated nanoTiO_2 epoxy composite films yielded more than 90% higher electrostatic energy storage density than the pure epoxy polymer.

Acknowledgements

This work was made possible by the funds provided by the DST-SERB Start-Up research grant for young scientists (No. SB/FT/CS-019/2012), Government of India. We would like to acknowledge the micro and nano characterization facility of the centre for nano science and engineering and the materials research centre, Indian Institute of Science, Bangalore, for providing XPS, FE-SEM and nanodielectrics impedance characterizations.

References

[1] Chu B, Zhou X, Ren K, Neese B, Lin M, Wang Q *et al* 2006 *Science* **313** 334
[2] Li J Y, Zhang L and Ducharme S 2007 *Appl. Phys. Lett.* **90** 132901
[3] Muralidhar C 1988 *Jpn. J. Appl. Phys.* **27** 1349
[4] Xiaojun Y, Zhimin Y, Changhui M and Jun D 2006 *Rare Metals* **25** 250
[5] Cao Y, Irwin P C and Younsi K 2004 *IEEE Trans. Dielectr. Electr. Insul.* **11** 797
[6] Ciuprina F, Plesa I, Notingher P V, Tudorache T and Panaitescu D 2008 *Annual Report Conference on Electrical Insulation and Dielectric Phenomena*, October 26–29, Quebec p 682
[7] Kim P, Jones S C, Hotchkiss P J, Haddock J N, Kippelen B and Marder S R 2007 *Adv. Mater.* **19** 1001
[8] Ramesh S, Shutzberg B A, Huang C, Gao J and Giannelis E P 2003 *IEEE Trans. Adv. Packag.* **26** 17
[9] Bai Y, Cheng Z Y, Bharti V, Xu H S and Zhang Q M 2000 *Appl. Phys. Lett.* **76** 3804
[10] Liang S, Chong S R and Giannelis E P 1998 In *Proceedings of the 48th Electronic Components and Technology Conference*, May 25–28, Seattle, Washington, USA
[11] Roy M, Nelson J K, MacCrone R K, Schadler L S, Reed C W, Keefe R *et al* 2005 *IEEE Trans. Dielectr. Electr. Insul.* **12** 629
[12] Gilbert L J, Schuman T P and Dogan F 2005 In *Ceramic transactions series: advances in electronic and electrochemical ceramics*, F Dogan and P M Kumta (eds) (Baltimore: Wiley) **179** p 17
[13] Schuman T P, Siddabattuni S, Cox O and Dogan F 2010 *Compos. Interface* **17** 719
[14] Hosokawa M, Nogi K, Naito M and Yokoyama T 2007 *Nanoparticle technology handbook* (Oxford, UK: Elvesier)
[15] Siddabattuni S, Schuman T P and Dogan F 2013 *ACS Appl. Mater. Interfaces* **5** 1917
[16] Siddabattuni S, Akella S H, Gangula A and Patnaik S 2015 *Bull. Mater. Sci.* **38** 1399
[17] Siddabattuni S, Schuman T P and Dogan F 2011 *Mater. Sci. Eng. B* **176** 1422
[18] Helmy R and Fadeev A Y 2002 *Langmuir* **18** 8924
[19] Grest G S and Cohen M H 1981 *Adv. Chem. Phys.* **48** 455
[20] Chen H M, Lee L J, Yang J T, Gu X and Jean J C 2009 *Mater. Sci. Forum* **607** 177
[21] Blum F D, Sinha B R and Schwab F C 1990 *Macromolecules* **23** 3592
[22] Blum F D, Lin W Y and Porter C E 2003 *Colloid. Polym. Sci.* **281** 197
[23] Barber P, Balasubramanian S, Anguchamy Y, Gong S, Wibowo A and Gao H 2009 *Materials* **2** 1697
[24] Ma D, Siegel R W, Hong J I and Schadler L S 2004 *J. Mater. Res.* **19** 857
[25] Tuncer E, Sauers I, James D R, Ellis A R, Paranthaman M P, Aytug T *et al* 2007 *Nanotechnology* **18** 25703
[26] Macomber R 1996 *Organic chemistry* Vol 1 (California: University Science Books) p 275
[27] Chester T L and Pinkston J D 2005 In *Analytical instrumentation handbook*, J Cazes (ed), 3rd edn (New York: Marcel Dekker) Chapter 24, p 759